

Frictional Properties of the Micro-Textured Surface of Anisotropically Etched Silicon

N. Moronuki, Y. Furukawa (1)

Graduate School of Mechanical Engineering, Tokyo Metropolitan University, Tokyo, JAPAN

Abstract

Anisotropic etching of silicon produces regular shapes that consist of $\{111\}$ crystal planes. Applying a line-and-space mask pattern, textured surfaces with periodic regular shapes such as V-grooves are easily obtained. This paper first describes the design principle for such textures. By choosing an appropriate crystal orientation, symmetric or asymmetric grooves can be obtained. Variation of the texture profile is also discussed. The frictional properties are then examined. The effects of the texture were: (1) friction could be decreased, and (2) frictional directionality could be obtained with a combination of asymmetric texture and softer materials.

Keywords:

Texture, Friction, Anisotropic etching

1 INTRODUCTION

Various functions can be obtained from the surface texture, which is defined as a regular microstructure periodically placed on the surface, and its application is under exploitation [1]. A wide spectrum of processes are used for texturing from conventional machining to energy-beam processing [2], including crystal growth [3]. Application fields are also widespread from traditional machinery to the IT industry [4] and MEMS devices [5]. Requirements for these processes are, of course, low cost as well as accuracy and repeatability.

The anisotropic etching of silicon (Si) produces specific regular shapes with good repeatability depending on the crystal structure [6]. Single crystal silicon can be used as the structural material after processing because of its good mechanical properties with few internal defects. If the brittleness of silicon causes any problem, the texture can be transferred to other structural materials by replication process. Replication is one of the most cost effective processes.

On the other hand, the effect of the surface microstructure on friction has been elucidated in the field of the forming process [7,8,9]. In the field of micro-mechanisms, texture is often applied to reduce the adhesion force [10]. However, there are few studies of sliding friction in micro-mechanisms though some of the friction mechanisms at the atomic level have been clarified using scanning probe microscopy [11].

In this paper, the texture design that applies anisotropic etching to silicon is discussed first. Then, the frictional properties are clarified with particular emphasis on the directionality of the friction.

2 DESIGN AND PRODUCTION OF TEXTURE

2.1 Principle and design

The typical shape produced by anisotropic etching of silicon consists of $\{111\}$ planes because the etching rate against this plane is the minimum. When a line-and-space mask aligned along $\langle 110 \rangle$ on a (110)-orientation

substrate is used, the final shape becomes a symmetric V-groove the opening angle of which is 109.5 degrees as shown in Figure 1(a). In the figure, the crystal lattice is also shown to aid understanding. If the substrate (221)- or (331)-orientation is chosen, an asymmetric V-groove with the same opening angle can be obtained as shown in Figure 1(b).

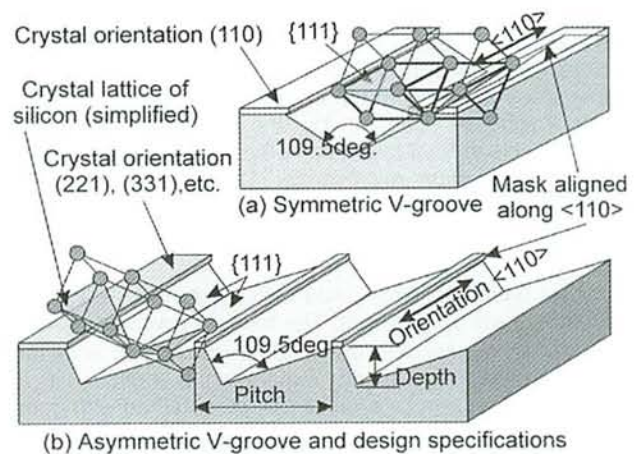


Figure 1: Crystal lattice and the principle of texturing.

Table 1 summarizes the possible cross-sections of the texture that are obtained with this process. By choosing both the substrate orientation and the mask orientation, various textures can be obtained, where the opening angle of the groove is typically limited to 70.5 or 109.5 degrees that consist of $\{111\}$ planes. A parallel wall is also possible, where the obtained orientation is not $\{111\}$ but $\{100\}$ against which the etching rate is not the minimum but the maximum. Thus, in this case, the etching time should be strictly controlled to obtain accurate dimensions.

In Table 1, both V-shapes with 70.5 and 109.5 degrees are shown. The angle is determined by assuming the $\langle 110 \rangle$ crystal zone shown in the left of Figure 2, and all

of the crystal planes are projected as lines in the αz plane. On this plane, the set of crystal planes $\{111\}$ form a parallelogram. The opening angle is determined by the combination of $\{111\}$ planes that easily appears along with the advance of the etching. Thus, if the Miller index of the crystal plane before etching $[11\gamma]$ satisfies the condition $\gamma < 1$, for example the $\{221\}$ plane, then the opening angle of the groove becomes 109.5 degrees. On the other hand, if $\gamma > 1$, for example $\{112\}$, then the opening angle becomes 70.5 degrees.

The obtainable profile is limited to V or rectangular because the regularity of the crystal lattice is utilized. Instead, the design becomes simple. If the etching rate against the $\{111\}$ planes is negligible, the symmetric property is determined only by the orientation of the substrate, while the depth of the groove is determined by the orientation and the pitch of the mask. The etching time is estimated from the depth and etching rate against each orientation.

2.2 Production of the texture

The oxide layer of the silicon substrate was used as the etching mask. The line-and-space mask patterns were transferred on it using photolithography. The width of both the line and the space was $3\mu\text{m}$ or $6\mu\text{m}$. The whole size of the pattern was 30mm by 60mm and etched substrate was cut into small pieces of which size is 10mm by 10mm for the evaluation of frictional properties. Geometrical accuracy of the texture is directly affected by the error of the mask. The linearity error of the mask was less than $0.2\mu\text{m}$ and the pitch error was less than $0.5\mu\text{m}$. Etching conditions are shown in Table 2. The etching time was as short as 20 minutes because the etching depth was shallow.

Figure 3 shows the SEM photos and the cross-sectional profiles of the obtained texture. The orientation of the substrate is $(1.16\ 1.16\ 1)$ or (221) . The former orientation is a special one that has four degrees-offset from (111) plane. The profiles were measured with a confocal type microscope. The angle θ_1 shown in the figure almost coincides with the theory shown in Table 1, four degrees, though the opening angle does not coincide well. This error might be caused by the measurement error because it is difficult to measure the tilted smooth surface with confocal type microscope. The roughness of the obtained surface was about 20nm Ra. The typical waviness of the substrate before etching was less than $5\mu\text{m}$.

Another orientation (551) was also examined though the results are not shown here. The tendency was same with the former results and the angle θ_1 coincided with the theory. Based on these experimental results, it is concluded that regular profiles can be obtained with good geometrical accuracy and good roughness.

3 MEASUREMENT OF FRICTION

3.1 Experimental set-up

Figure 4 shows the experimental setup. Three quartz-type one-axis load sensors (resolution 0.5mN) were combined in a tripod structure and force components along the Cartesian coordinates were measured. Flexure hinges at both ends of the force sensor absorbed the misalignment between the specimens and assured steady and uniform contact between them. Force components along each axis were calculated from the geometrical relationship. The nominal resolution and capacity in each direction are shown in the figure. The drift of the output was less than 5mN for three minutes, while the typical measurement time was about three

	Crystal orientation	Mask orientation	Cross-Section Appearance	θ_1, θ_2	
				θ_1 (deg)	θ_2 (deg)
-	$\{100\}$	$\langle 110 \rangle$		54.7	70.5
		$\langle 100 \rangle$		90	-
0	$\{110\}$	$\langle 110 \rangle$		35.3	109.5
		$\langle 111 \rangle$		54.7	-
>1	$\{112\}$	$\langle 110 \rangle$		19.5	70.5
	$\{113\}$	$\langle 110 \rangle$		29.5	70.5
	$\{114\}$	$\langle 110 \rangle$		35.3	70.5
<1	$\{1.16\ 1.16\ 1\}$	$\langle 110 \rangle$		4	109.5
	$\{221\}$	$\langle 110 \rangle$		15.8	109.5
	$\{331\}$	$\langle 110 \rangle$		22	109.5

Table 1: Variation of the texture cross-section.

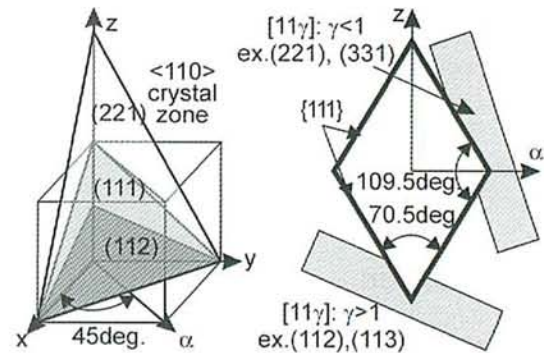


Figure 2: Crystal orientation and obtained V-angle.

Etchant	Potassium hydroxide (KOH)
Concentration	35wt%
Temperature	333K
Additive	Isopropyl alcohol (IPA) saturated

Table 2: Etching conditions.

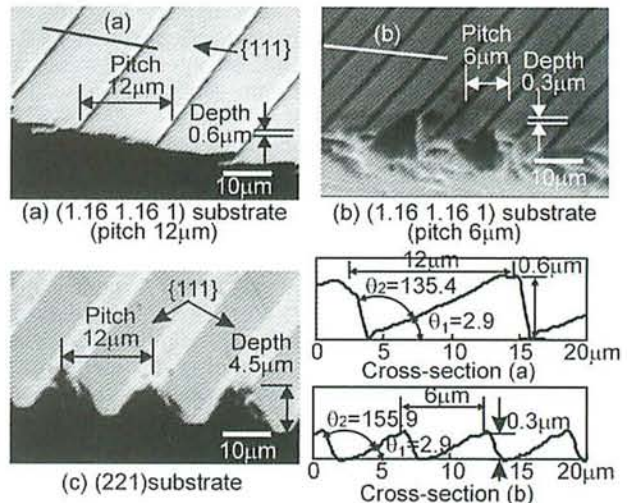


Figure 3: SEM photo and cross-sectional profile of the texture.

minutes. The natural frequency in the Z direction was 155Hz.

Motion between the specimens was applied with the XY stage controlled by a PC. Each axis was driven by a linear motor with $0.1\mu\text{m}$ feedback scale, and main reciprocation was applied in X direction. Contact

pressure between the specimens was adjusted by the position of a weight above the over-arm, which was controlled by a linear motion stage. The drive direction in XY plane was adjusted with a rotary table on the XY stage, though it is not shown in the figure. The experiments were carried out in a normal environment.

3.2 Basic properties

Figure 5 shows the friction between the textured Si and planar Si. The textured Si has asymmetric grooves with a $6\mu\text{m}$ -pitch as shown in Figure 3(b). The friction force during two reciprocations of 1.5mm travel was measured continuously. The inclined parts of the graph at the beginning and the reverse point of the feed were due to the elastic deformation of the structure and workpiece. It was found from this result that steady motion was applied and the average friction forces in both directions were the same in spite of a fluctuation of about 14mN .

In the following experiments, some conditions were kept constant for the convenience of comparison. The size of the testpiece was 10mm by 10mm . It was cleaned ultrasonically with ethanol, then with pure water and dried with nitrogen gas. The sliding speed was $30\mu\text{m/s}$, and all of the measurements were completed in one hour.

Figure 6 shows the relationship between the contact pressure and friction in various combinations of silicon surfaces. The combination involved two plane contacts, parallel or perpendicular to the textured surfaces shown in Figure 3(b). In every case, the friction increased with decrease in contact pressure, which was especially remarkable in the case of the plane contacts. The reason for the increase in friction is considered to be the strong adhesion force due to water capillary at the asperities in the real contact area, which often constricts the motion of micro-mechanisms. In the case of the combination of textured surfaces, the increase in friction with decrease in contact pressure was small. Especially, the friction was almost constant in the case of perpendicular contact. In this combination, the real contact area became the minimum, thus the adhesion force also became the minimum.

Figure 7 also shows the relationship between the contact pressure and friction, where two planes with different crystal orientations were placed in contact. In this case, the size of testpiece was large and contact pressure was low. The tendency for the friction to increase with decrease in contact pressure was the same with the former results. However, the effect of crystal orientation is observed. In the case of the (100) substrate, the friction became smaller though the surface was smoother and the real contact area was larger than that of the (111) substrate. The surface energy of the (100) crystal plane is 1.99J/m^2 and larger than that of the (111) plane 1.15J/m^2 . Thus it is active and may have adsorbed various substances such as contaminants. The difference in such surface properties might have caused the difference in friction.

3.3 Frictional directionality by texturing

Figure 8 shows the results of similar experiments except that the asymmetric textured Si and different materials were made in contact. The textured silicon slid on the polypropylene plate. The Young's modulus of the polypropylene was $3.0\text{--}3.3\text{GPa}$, while that of the silicon was 187GPa . It is found that the appearance of the graph is almost same with that in Figure 5 but there is a frictional offset, which means that the friction in the forward direction is 42mN smaller or larger than that in the reverse direction. Compared with the results of Figure 5, the difference in this case was obviously caused by the asymmetric texture whereas in the former case the friction pattern had perfect symmetry.

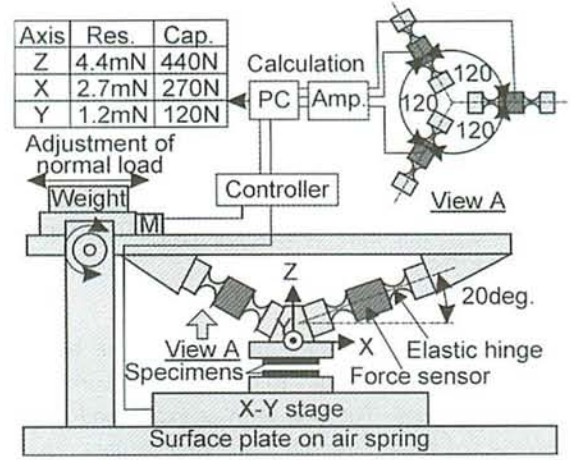


Figure 4: Arrangement for the friction measurements.

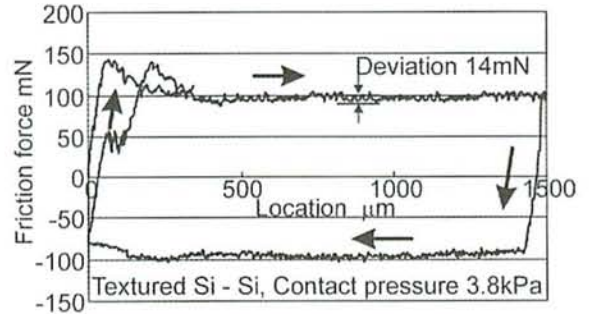


Figure 5: Example of friction measurement (Si-Si).

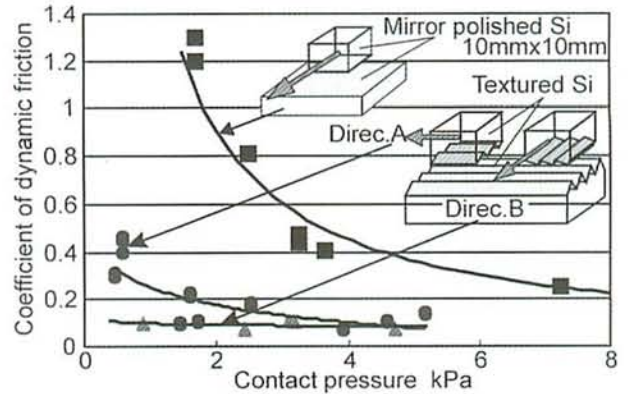


Figure 6: Effect of the texture pattern.

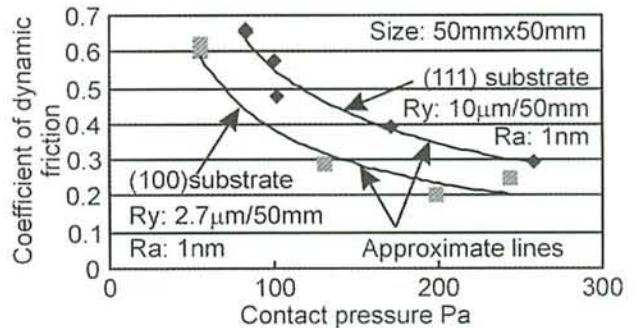


Figure 7: Effect of substrate orientation.

Figure 9 shows the case of the textured silicon and paper combination. The Young's modulus of the paper was $0.2\text{--}0.5\text{GPa}$. The friction pattern became the offset parallelogram again. The difference between the friction forces in each direction became as large as 111mN and their ratio is about three. In this case, the stick-slip motion was observed before reaching the steady sliding

motion. The slope at the reversing points is gentle compared with the former results. This slope is caused by the elastic deformation of the system as mentioned above, and the deformation of the paper has become as large as about 400 μ m because of low Young's modulus.

Figure 10 shows the effect of contact pressure on frictional directionality, which is defined as the ratio of the friction in each direction. It is found that the directionality is almost constant in this pressure range. The friction f_r can be assumed to be:

$$f_r = f_a + f_g \quad (1)$$

where f_a is the force necessary to shear the adhesion and f_g is the force necessary to carry out the work to slide over the asperities. The first term is expressed as sA_r , the product of shear strength s and real contact area A_r .

The second term is same with the Amonton's theory that assumes no plastic deformation such as ploughing and is expressed as $W \cos \theta_1$, where W is the normal force and θ_1 is the slope angle as shown in Table 1. This theory can be applied because the contact pressure was low and no surface damage was observed after the experiment. In the case of the combination with softer materials, the first term becomes negligible because of the low shear strength, and the second term becomes predominant. Thus, frictional directionality can be explained by the asymmetric geometry of the texture.

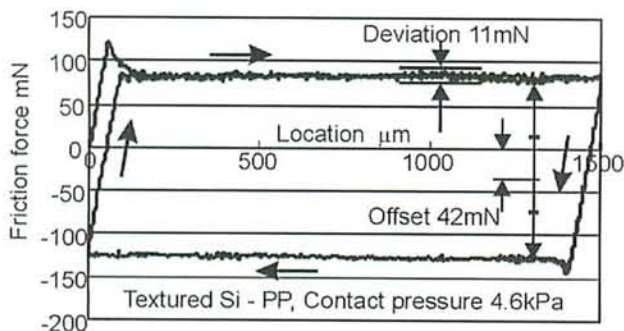


Figure 8: Friction between textured Si and polypropylene.

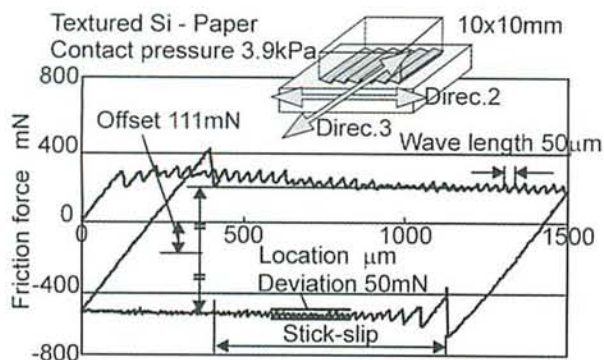


Figure 9: Friction between textured Si and paper.

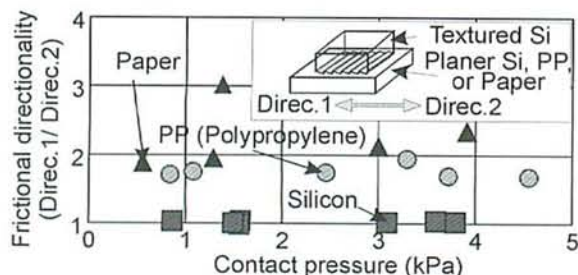


Figure 10: Effect of material combination

4 CONCLUSIONS

The application of anisotropic etching of silicon to texturing was proposed and the frictional properties of the textured surface were examined. The results are summarized as follows:

- (1) The design of the texture profile, which applies the anisotropic etching of silicon, has been elucidated.
- (2) Texture can decrease the increase in friction at low contact pressure.
- (3) Frictional directionality can be obtained in the combination of asymmetric texture and materials with different Young's modulus. In the case of the combination of textured silicon and polypropylene, the friction in one direction was about twice of that in the other direction.

5 REFERENCES

- [1] Evans C. J., Bryan J. B., 1999, "Structured", "textured" or "engineered" surfaces, *Annals of CIRP*, 48/2:541-556.
- [2] Zaidi S. H, Ruby D. S. and Gee J. M., 2001, Characterization of Random Reactive Ion Etched-Textured Silicon Solar Cells, *IEEE Trans. Elec. Dev.*, 48/6: 1200-1206.
- [3] Kakuta A., Moronuki N., Furukawa Y., 2002, Nano-Texturing of Surfaces by Constricting Epitaxial Growth of Molecules, *Annals of CIRP*, 51/1: 323-326
- [4] Yanagi K., Kobayashi Y., 1993, Surface texture assessment in the tangential direction of a rigid magnetic disk to reduce the friction force between head and disk surface, *IEEE Trans Magnetics*, 29, 6 Pt 2: 3951-3953.
- [5] Kim J., Kim C.J., 2002, Nanostructured surfaces for dramatic reduction of flow resistance in droplet-based microfluidics, *IEEE MEMS Conf*: 479-482.
- [6] Moronuki N., 1999, Linear Motion Microsystem Fabricated on a Silicon Wafer, *Int. J. Japan Soc. Prec. Eng.*, 33, 2: 83-86.
- [7] Balbach R., Lange K., 1987, Influence of various surface microstructures on the tribology in aluminium sheet metal, *Annals of CIRP*, 36/1:181
- [8] Azushima A., Miyamoto J., Kudo H., 1998, Effect of surface topography of workpiece on pressure dependence of coefficient of friction in sheet metal forming, *Annals of CIRP*, 47/1: 479.
- [9] Pfestorf M., Engel U., Geiger M. 1998, 3D Surface Parameters and their Application on Deterministic Textured Metal Sheets, *Int. J Mach Tools Manuf.*, 38, 5/6: 607.
- [10] Yee Y., Chun K., Lee J. D., 1995, Polysilicon surface modification technique to reduce sticking of microstructures, *Proc. 8th Int. Conf. Solid-State Sensors and Actuators*: 206.
- [11] Bhushan B., 1999, *Handbook of micro/nano tribology*, CRC press.